Spectrochimica Acta Part A: Molecular and Biomolecular Spectroscopy 252 (2021) 119522

Contents lists available at ScienceDirect

Spectrochimica Acta Part A: Molecular and Biomolecular Spectroscopy

journal homepage: www.elsevier.com/locate/saa

Quality evaluation of Keemun black tea by fusing data obtained from near-infrared reflectance spectroscopy and computer vision sensors

Yan Song [a], Xiaozhong Wang [a], Hanlei Xie [a], Luqing Li [b], Jingming Ning [b,*], Zhengzhu Zhang [b]

[a] School of Engineering, Anhui Agricultural University, Hefei 230036, China
[b] State Key Laboratory of Tea Plant Biology and Utilization, Anhui Agricultural University, Hefei 230036, China

HIGHLIGHTS

- A method combing NIRS and a computer vision system were proposed in this study.
- The method (a sensor fusion strategy) is used for grading Keemun black tea.
- A CNN model was constructed to extract NIRS features.
- The accuracy of the proposed strategy was higher than that of a single-sensor strategy.
- The sensor fusion strategy nearly attained 100% in grading black tea samples.

GRAPHICAL ABSTRACT

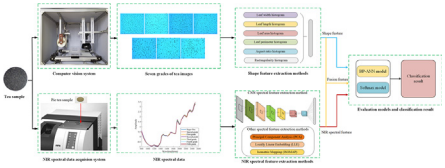

ARTICLE INFO

Article history:
Received 20 July 2020
Received in revised form 19 January 2021
Accepted 20 January 2021
Available online 2 February 2021

Keywords:
Keemun black tea
Near-infrared reflectance spectroscopy
Computer vision system
Feature fusion
Convolutional neural network
Quality identification

ABSTRACT

Keemun black tea is classified into 7 grades according to the difference in its quality. The appearance and flavour are crucial indicators of its quality. This research demonstrates a rapid grading method of jointly using near-infrared reflectance spectroscopy (NIRS) and computer vision systems (CVS) to evaluate the flavour and appearance quality of tea. A Bruker MPA Fourier Transform near-infrared spectrometer was used to record the spectrum of samples. A computer vision system was used to capture the image of tea leaves in an unobstructed manner. 80 tea samples for each grade were analyzed. The performance of four NIRS feature extraction methods (principal component analysis, local linear embedding, isometric feature mapping, and convolutional neural network (CNN)) was compared in this study. Histograms of six geometric features (leaf width, leaf length, leaf area, leaf perimeter, aspect ratio, and rectangularity) of different tea samples were used to describe their appearance. A feature-level fusion strategy was used to combine softmax and artificial neural networks (ANN) to classify NIRS and CVS features. The results indicated that for an individual NIRS signal, CNN achieved the highest classification accuracy with the softmax classification model. The histograms of the combined shape features indicated that when the softmax classification model was used, the classification accuracy was also higher than ANN. The fusion of NIRS and CVS features proved to be the optimal combination; the accuracy of calibration, validation and testing sets increased from 99.29%, 96.67% and 98.57% (when the optimal features from a single-sensor were used) to 100.00%, 99.29% and 100.00% (when features from multiple-sensors were used). This study revealed that the combination of NIRS and CVS features can be a useful strategy for classifying black tea samples of different grades.

* Corresponding author.
E-mail address: ningjm1998009@163.com (J. Ning).

https://doi.org/10.1016/j.saa.2021.119522
1386-1425/

1. Introduction

Keemun tea, Assam tea, Darjeeling tea, and Ceylon tea are prominent types of black tea worldwide and have excellent quality [1]. Tea quality considerably affects the market price of and consumer satisfaction with a tea product. Therefore, tea quality control is essential. In general, the appearance (an external indicator) and chemical composition (an internal indicator) of tea are the main indicators of tea quality. The traditional method for assessing the quality of black tea is organoleptic evaluation. In this method, experts grade the quality of tea samples on the basis of the samples' appearance, aroma, liquor colour, and taste. However, this method is subjective [2]. Although gas chromatography-mass spectrometry (GC–MS) or liquid chromatography-mass spectrometry (LS-MS) is an objective assessment procedure, both procedures involved a complex process for detecting the chemical components of tea [3,4]. Accordingly, an objective and intelligent evaluation method is required to replace organoleptic evaluation approaches. Among various nondestructive detection technologies, near-infrared reflectance spectroscopy (NIRS) and computer vision systems (CVSs) have been widely used.

Several studies have used NIRS and CVS technologies to assess the quality of many agricultural products, such as meat [5], honey [6], and fruit [7,8]. NIRS technology can be used to evaluate the quality of tea. NIRS data can reflect the content of amino acids, tea polyphenols, and other substances, which constitute the flavour quality of tea [9].

NIRS data are characterised by strong correlations and high redundancy. These characteristics bring a lot of problems with data processing. The method of NIRS feature extraction has become very important. Principal component analysis (PCA) can maximise the data structure characterisation of original variables without losing unrelated information. PCA has been extensively applied to NIRS data processing [10–12]. Local linear embedding (LLE) has been used to project high-dimensional data into a low-dimensional space and maintain the local linear relationship between data points. Huang et al. used an LLE algorithm to extract hyperspectral scattering features [13]. The isometric feature mapping (ISOMAP) method is developed on the basis of the multidimensional scaling (MDS) method, which requires all points in the space to participate in the construction of neighbourhood [14]. Mishra et al. used ISOMAP to extract the spectral features of six different commercial tea products [15]. These spectral feature extraction methods must be optimised individually to achieve an effective feature extraction scheme. Deep learning models based on convolutional neural networks (CNNs) can automatically extract complex and effective features from simple features. Therefore, such models been used extensively in the field of agriculture; for example, they have been used in plant disease recognition [16], weed identification [17], and crop pest classification [18]. In this study, a CNN was integrated with an NIR method for extracting the features of tea. The performance of this method was compared with that of PCA, LLE, and ISOMAP methods.

NIRS can identify the content distribution of the main quality components in tea, but cannot capture the appearance features of tea. Image information provided by CVSs can accurately and objectively reflect the appearance features of tea and plays a crucial role in tea quality evaluation. Relevant studies have applied several CVS techniques to evaluate the appearance of tea. For example, Gill, Kumar, and Agarwal used texture features to distinguish four different types of black tea [19]. Zhu et al. used image information as variables to evaluate the quality of tea [20]. In most of the aforementioned studies, texture features have been extracted after tea accumulation. Fineness and uniformity are crucial factors for grading the appearance of Keemun black tea. Accordingly, the present study introduced some geometric features to describe the shape characteristics of tea.

NIRS and CVS technology can obtain only the main component and external appearance of a sample, respectively, which is a partial and incomplete indication of tea quality. Therefore, to comprehensively evaluate tea quality, researchers have focused on multi-technology integration to address the drawbacks of using a single technology. Studies have executed data fusion by integrating data from multiple sensors. Miao et al. developed a hybrid system that could distinguish nine types of ginseng [21]. Kiani et al. developed an integrated system based on CVS and an e-nose for determining adulteration of saffron [22]. Accordingly, NIRS can be combined with a CVS to develop a data fusion strategy for evaluating the quality of black tea.

This study developed a nondestructive, objective, and precise method for determining the quality of black tea. This method involves the combination of a NIRS system and a CVS. We executed the NIRS system by applying four spectral feature extraction methods: PCA, LLE, ISOMAP, and CNN. We then compared the results obtained from each of the four spectral feature extraction methods in order to determine the ideal method for extracting the spectral features of black tea. We applied the CVS to extract the leaf shape features of black tea samples of different quality grades and then obtained shape histograms. Classification results obtained using NIRS features only, CVS features only, and combined NIRS and CVS features were compared. The technology roadmap is presented in Fig. 1.

2. Materials and methods

2.1. Sample materials

The samples were purchased from Yuansheng Tea Co., Ltd. at Qimen County of Anhui Province in December 2017, March 2018, and September 2018, respectively. According to the appraisal of the evaluation experts, the samples of Keemun black tea can be divided into seven grades: super fine, special grade, first grade, second grade, third grade, fourth grade, and fifth grade, with the reduction of its quality. 560 tea samples were prepared (80 samples for each tea grade). All tea samples were sealed and stored at 5 °C. After machine vision detection, each sample was transferred for near-infrared detection.

2.2. NIR spectral data acquisition

The NIR spectral data were recorded using a Bruker MPA Fourier Transform near-infrared spectrometer (Bruker Optik GmbH, Germany). Each spectrum is the average of 32 scans recorded between 800 and 2500 nm with a resolution of 2 cm^{-1}. The data were measured by 3.86 cm^{-1} interval, which resulted in 2203 data points (i.e. spectral variables) in each spectrum. The samples were ground to a powder and smashed to allow them to pass through 80 mesh filter screen (screen diameter less than 0.180 mm). For each sample, 3 ± 0.1 g of powders was compressed into a pie sample (30 mm diameter, 5 mm thickness) at a pressure of 20 MPa. A gold coated reference was used for background measurements when we start the spectrometer. The pie sample was paced on the PbS detector's detection area of NIRS instrument with an integrating sphere. In diffuse reflectance spectroscopy mode, the sample was measured thrice after 120° rotations. The mean spectra were calculated by using the OPUS 6.5 software package (Bruker, Germany) for further analysis.

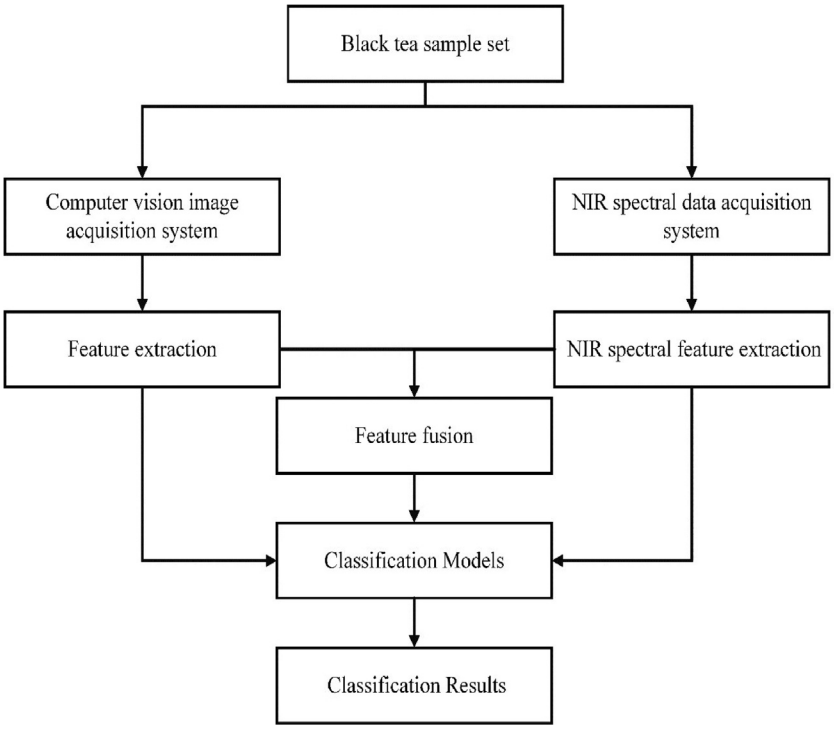

Fig. 1. Technology roadmap of evaluation of black tea quality.

2.3. Computer vision system set-up and image acquisition

The structure of the image acquisition system included an industrial camera, backlight, roller sieve, linear motion module, and carrier platform. First, the tea sample is loaded onto the roller sieve. Then, the linear motion module is activated, moving the carrier platform, while leaves fall through the sieve. In this manner, most of the leaves were evenly distributed on the platform in an unobstructed manner; the few leaves that overlapped with each other were separated manually. After this process, the industrial camera captures sample images. The camera used is MER500-14GM/C-P (Daheng image Co., Ltd., China), with a resolution of 2592 × 1944 and pixel size of 2.2 × 2.2 (μm × μm). There were also 80 pictures for each grade.

2.4. Data processing method and classification

2.4.1. NIR spectral and feature extraction

The pre-processing of raw spectral data is an essential step. Effective pre-processing can eliminate light scatter effects to a large extent [23]. In this study, the raw spectral data of the black tea samples were pre-processed using standard normal variate (SNV) transformation.

After pre-processing, further feature extraction and dimensionality reduction were performed. The spectral feature extraction and subsequent processing are shown in Fig. 2. A convolutional neural network (CNN) automatically learns the characteristic information at various scales through the convolution and pooling layer [24]. A typical CNN is composed of an input layer, convolution layer, pooling layer, and full connection layer. First, the input layer connects the input signal. Then, through the convolution operation of the local receptive field in the convolution layer, local features are extracted. The pooling layer is used to extract feature signals and reduce the dimensions. The full connection layer connects all previous layer feature maps [25]. The CNN extracts the spectral signals by eliminating redundant information, thus revealing underlying information in the spectral signals. Currently, there is no clear standard for the structure and parameters of a CNN model. After repeated experiments, we established an executable network to verify the feasibility of spectral feature extraction method based on CNN.

This network consisted of three convolution-pooling layers, a full connection layer, and an output layer for classification. The rectified linear unit (ReLU) was selected as the activation function [26]. Max-pooling was employed for this network. The first convolution layer, the second convolution layer, and the third convolution layer have kernels of sizes 204 × 1, 21 × 1, and 6 × 1, respectively. The number of convolutional kernels sequentially was 4, 8, and 16. The stride of the local receptive field in each convolution layer was 1. A wide convolutional kernel in the first convolutional layer can capture detailed spectral information. Then, a small convolutional kernel can capture more complex and more abstract information. The strides of the three max-pooling layers sequentially were set to 10, 6, and 5. Each node of the full connection layer was connected to the feature information in the upper layer. To avoid over-fitting and improve the generalization ability of the network, we added a dropout operation between the third pooling layer and the full connection layer. The probability of neuron dropout was 0.5 [27]. Finally, the softmax classifier or artificial neural network with back-propagation (BP-ANN) classifier was employed for classification. The detailed parameters of the CNN are listed in Table 1.

Other feature extraction methods, such as PCA, LLE, and ISOMAP, are widely used for dimension reduction. The basic idea of LLE is to approximate each data point by a linear combination of its neighbours and to find a low dimensional configuration of data points [28]. The number K of the nearest neighbours in LLE was specified to 12 in this study. ISOMAP approximates a neighbourhood graph by identifying K nearest neighbours for every data point [28]. The number K of its nearest neighbours was also specified to 12. ISOMAP and LLE methods were implemented in Matlab (R2018a, Mathworks, USA) using the Toolbox for Dimensionality Reduction (https://lvdmaaten.github.io/drtoolbox/).

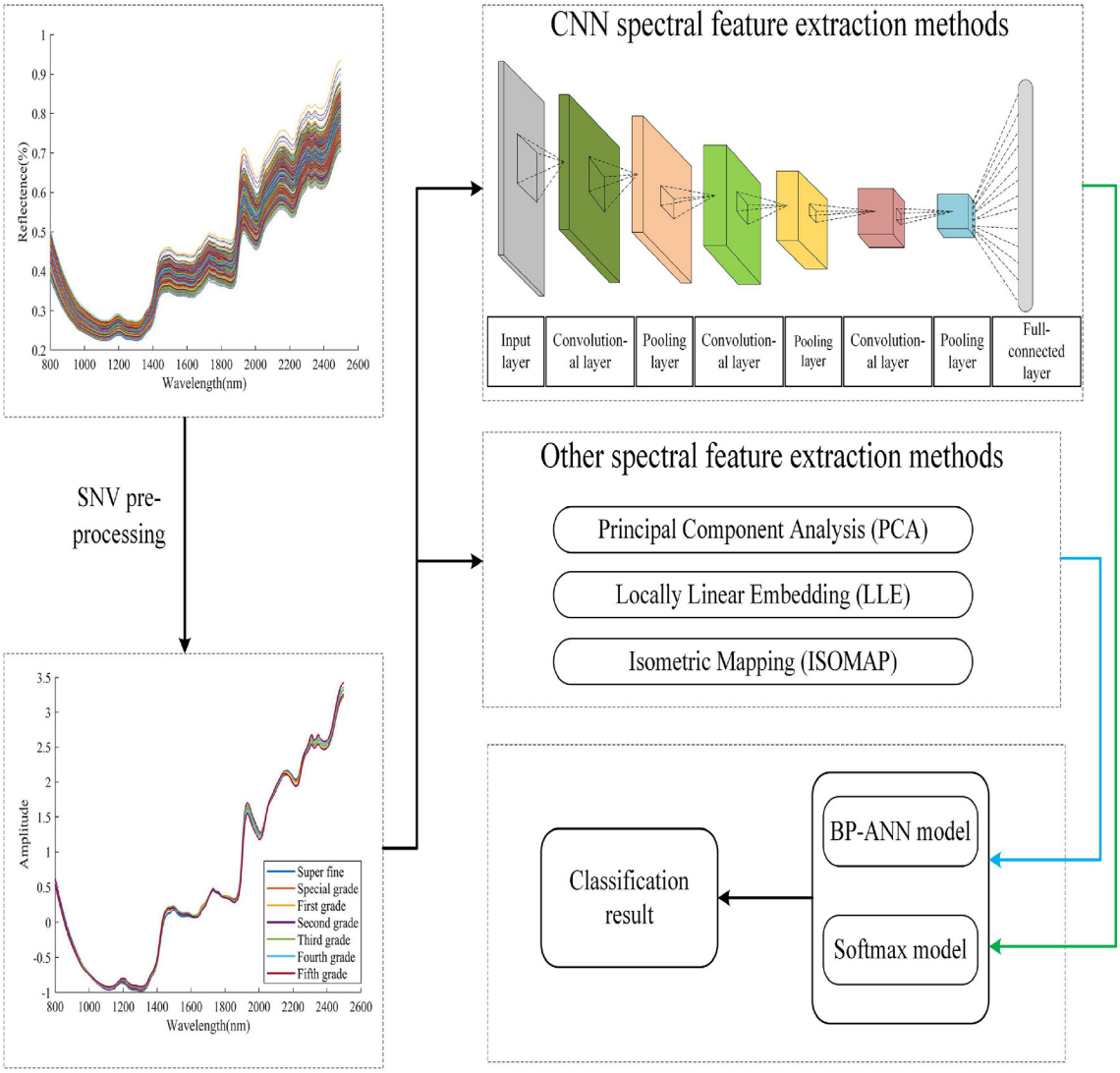

Fig. 2. Flow chart of spectral feature extraction and subsequent processing.

Table 1
Structural parameters of the designed convolutional neural network.

No. layer	Layer type	Kernel size (Stride)	Kernel number	Output size
1	Convolution	204 × 1(1)	4	2000 × 1
2	Max Pooling	10 × 1(10)	4	200 × 1
3	Convolution	21 × 1(1)	8	180 × 1
4	Max Pooling	6 × 1(6)	8	30 × 1
5	Convolution	6 × 1(1)	16	25 × 1
6	Max Pooling	5 × 1(5)	16	5 × 1
7	Dropout	0.5	/	80 × 1
8	Fully connected	80	/	80 × 1
9	Classifier	7	/	7 × 1

2.4.2. CV image acquisition device and feature extraction

The leaf shape feature was extracted from the image. The flow chart of the algorithm for leaf feature extraction is shown in Fig. 3. First, an RGB image was converted to a grey image. Second, a threshold value was chosen using Otsu's method [29], after which the grey image was converted into a binary image. Third, the noise was reduced using a median filter [30]. Using the above-mentioned processing procedure, we separated the leaves from the background in the image. The shape feature of the leaves could be extracted [31].

Six leaf shape features (leaf length, leaf width, leaf area, leaf perimeter, aspect ratio, and rectangularity) are introduced; these features are defined as follows:

(i) Leaf width: the average width of the leaves, denoted by *W*.
(ii) Leaf length: the skeleton line length in the leaf image, denoted by *L*.
(iii) Leaf area: the number of pixels on the binary image of the leaf, denoted by *A*. Every leaf has area characteristics, which occupy the pixel space.

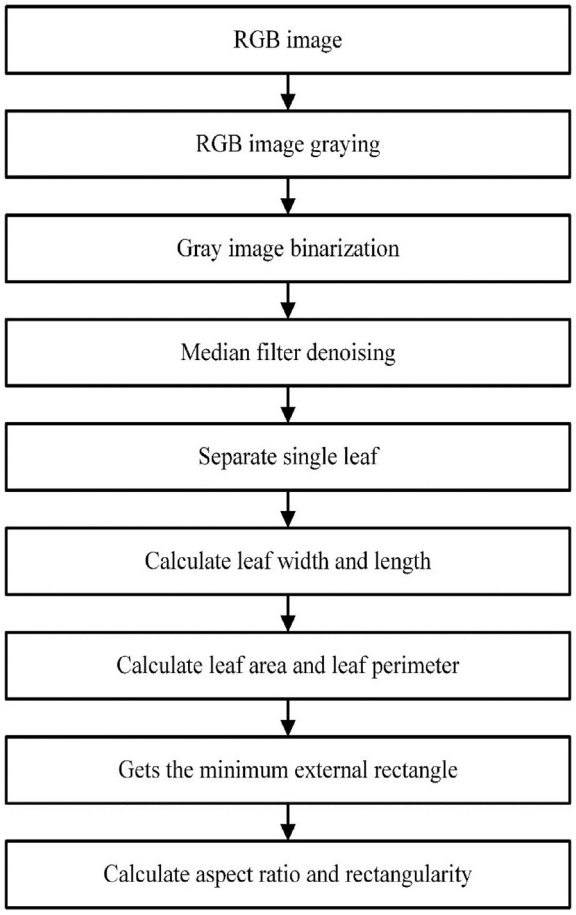

Fig. 3. Flow chart of the image processing algorithm.

(iv) Leaf perimeter: calculated by counting the number of pixels that lie on the boundary of the binary image of the leaf.
(v) Aspect ratio: the ratio of leaf length to leaf width $AR = \frac{L}{W}$. Aspect ratio is denoted by *AR* and is an important characteristic.
(vi) Rectangularity: measure of the degree of similarity between a rectangle and the leaf shape or simply the match level between leaf shape and a rectangle. It is calculated using $\frac{A}{L \times W}$.

The appearance features of Keemun black tea are determined according to the distribution trend of all leaf shape features. Therefore, we scaled each geometric feature into several ranges and counted the shape distribution frequency of leaves that fall into each range. The number of bin ranges of the leaf width, leaf length, leaf area, leaf perimeter, aspect ratio, and rectangularity was 12, 16, 16, 18, 18, and 12, respectively. Then, the histograms of the shape features were obtained [32,33]. According to the order of leaf width, leaf length, leaf area, leaf perimeter, aspect ratio, and rectangularity, these six leaf shape features were successively connected into a histogram of 92 variables. These histograms were then used to describe the appearance features of the sample.

2.4.3. Data fusion strategy

Here, we describe the data fusion stage. Data fusion can be divided into three different levels: data-level, feature-level, and decision-level [34]. In data-level fusion, directly combining a CVS and NIRS is difficult because they are two different sensors with heterogeneous data. Thus, they are unsuitable for data-level fusion. In decision-level fusion, multi-step data learning should be performed from raw data to the last decision. Furthermore, this procedure may lead to a significant loss of information. In this study, we adopted feature-level fusion for the spectral features and shape features to classify the tea grade. In feature-level fusion, NIRS feature was extracted from NIRS data with the methods in Section 2.4.1, which was a one-dimensional NIRS feature vector. The histograms of leaf shape features mentioned in Section 2.4.2 were used as the appearance feature, which was a one-dimension vector. These two feature vectors were merged into a single vector for further analysis.

2.4.4. Classification models

Two classification models were chosen to distinguish between the different grades of the tea sample. The first of these models was BP-ANN. This model is widely used for modelling, classification, and optimization via input, hidden, and output layers to imitate the functions of the human brain [35]. In this study, the number of neurons in the input layer was equal to the length of the input feature vector. The number of neurons in the hidden layers was set to ten after fine-tuning. The output layer had seven neurons, which is equal to the number of tea grades. The tangent sigmoid function was chosen as the activation function. The initial weight values that connected these layers were generated randomly and updated after every training epoch according to the gradient descent function. The mean squared error (MSE) function was chosen as the cost function.

The softmax model, which is a generalization of the logistic model of multi-classification problems [36], was chosen as the comparative classification model in this study. Given a training dataset of k classes, where the input features are $x^i \in \{1, 2, 3, \cdots\cdots, k\}$, the hypothesis is

$$y = \begin{bmatrix} p(y^{(i)} = 1|x^{(i)};\theta) \\ p(y^{(i)} = 2|x^{(i)};\theta) \\ \cdots \\ p(y^{(i)} = k|x^{(i)};\theta) \end{bmatrix} = \frac{1}{\sum_{j=1}^{k} \exp(\theta_j^T x^{(i)})} \begin{bmatrix} \exp(\theta_1^T x^{(i)}) \\ \exp(\theta_2^T x^{(i)}) \\ \cdots \\ \exp(\theta_k^T x^{(i)}) \end{bmatrix}$$

where θ denotes the weight matrix of all model parameters, and y is the result of the classification. The cross-entropy cost function of calculating θ is

$$J(\theta) = -\frac{1}{m}\left[\sum_{i=1}^{m}\sum_{j=1}^{k}\{y^{(i)} = j\} log \frac{\exp(\theta_j^T x^{(i)})}{\sum_{j=1}^{k}\exp(\theta_j^T x^{(i)})}\right]$$

The parameter vector θ is adjusted by the gradient descent method, so that the cross-entropy cost function $J(\theta)$ reaches the minimum value quickly to improve the classification accuracy [37].

560 samples (80 samples each grade) were applied in this study, both in NIR spectral and CV images. The samples were divided into training set and testing set randomly. 420 samples (60 samples each grade) were used for training set, and 140 samples (20 samples each grade) were used for testing set. The original training set was split into internal calibration and validation sets randomly. The 5-fold cross-validation is applied to the training sets to calibrate model and optimize parameters. The accuracy of the classification model was computed using the following expression

$$accuracy\% = \left(\frac{number\ of\ correctly\ classified\ samples}{total\ number\ of\ samples}\right) \times 100$$

3. Results and discussion

3.1. Spectral data feature description

The original spectra obtained from the tea samples are displayed in Fig. 4(a). Original spectral could be easily affected by

noise signals, such as high-frequency noise, baseline drift, and light scattering. To reduce the influence of noise signals, original spectral curves should be processed using the SNV method. The average spectra derived for tea sample for each grade after pretreatment was shown in Fig. 4(b). As illustrated in Fig. 4(b), the spectrograms of the tea samples of different grades were similar. The NIR spectral of tea samples mainly represent functional groups related to carbohydrates, polyphenols, caffeine, amino acids, and proteins present in the samples. These features commonly appear in the NIR spectra of tea acquired using diffuse reflectance techniques and have been reported in the spectra of oolong, black, and green tea samples [38–40]. In this study, the average spectra derived for tea sample for each grade after pretreatment (Fig. 4(b)) revealed that the stretching and bending vibrations of various functional groups (e.g. C—H, O—H, and C—O) related to the content of endoplasmic components considerably affected the NIR spectral trend [41]. The study revealed absorption bands at 1350–1375 nm, which could be attributed to the first-order frequency doubling of the C—H group [42]. In addition, absorption bands were observed at 1800–1900 nm and were attributed to the C—O group [42]. Finally, absorption bands were observed at 1380–1420 and 1900–2000 nm and were ascribed to the O—H group [43].

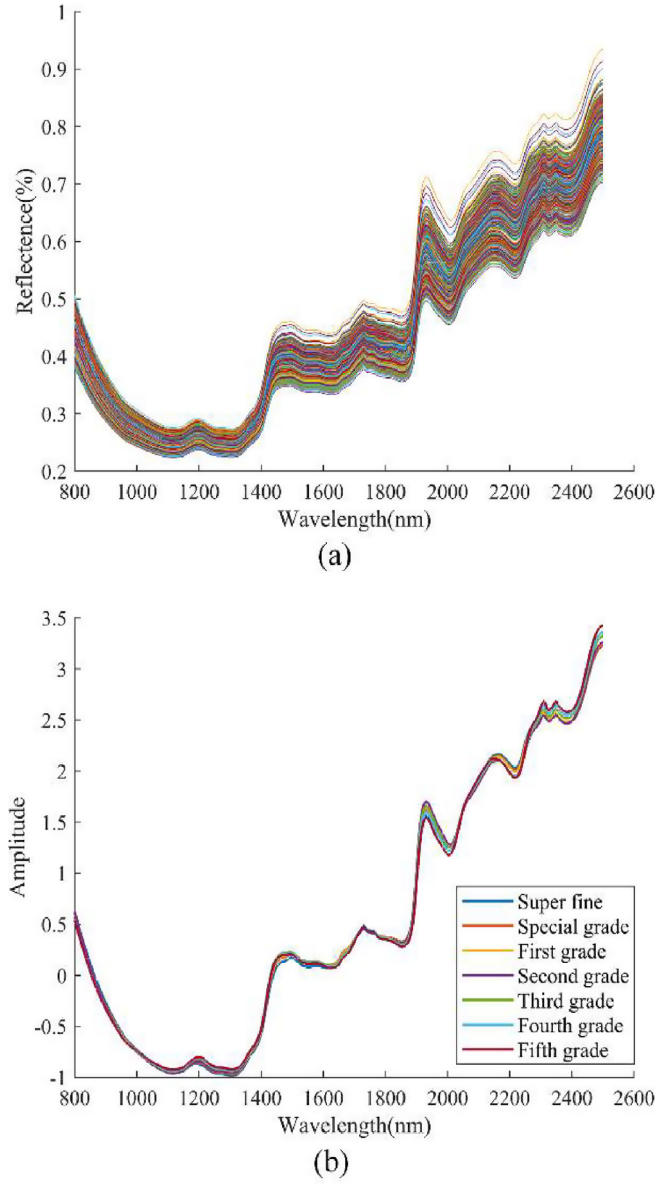

Fig. 4. NIR spectral curves, (a) original NIR spectral curves, (b) average spectral curves of each grade sample after SNV preprocessed.

3.2. Classification results with different feature extraction methods

In this study, four feature extraction methods were compared to establish reliable discrimination model of Keemun black tea. To reduce redundancy, the NIRS feature data set was processed using these methods. The features dimensionality (FD) also had a great influence to the classification result. For a given set of feature dimensionality (FDs = 10, 20, 30, 40, 50, 60, 70, 80, 90, 100), the FDs that gave the maximum mean accuracy rate of 5-fold cross validation sets were selected as the optimal dimensionality. In all spectral feature extraction methods, the spectral feature with the highest extraction accuracy was extracted for further analysis.

The 5-fold cross validation accuracy of two classification models according to the number of features dimensionality were shown in Fig. 5. Classification accuracy of four spectral feature extraction methods with the optimal FDs was shown in Table 2. As seen in Fig. 5, irrespective of the classifier used, or how the feature dimension changed, the classification accuracy for the calibration set was higher than that for the 5-fold cross validation when using ISOMAP for feature extraction. This is an over fitting phenomenon. ISOMAP utilises the geodesic distance accounting for the non-linearity in the high dimensional data manifold. The reason for the poor performance of ISOMAP is that as the emergence of new data from the validation set, the optimal geodesic distance could not be found for the validation set with the parameters derived from the calibration set. While the accuracy for the testing set was also reduced. Some other weakness of ISOMAP was also discussed in relate study [15,44,45].

When using the LLE method, we can also find, no matter what classifier was used, the classification accuracy for the calibration set was higher than that for 5-fold cross validation. The LLE method reconstructed information through the neighbouring points. Many studies have shown that the organic compounds in tea samples have unique spectral fingerprints in the NIR spectrum [40]. These spectral fingerprints generally comprise several spectral absorption bands of hydrogen-containing functional groups. Tea quality is not determined by neighbouring points but by several absorption bands, which may be the main reason why the results of LLE classification are no high.

As a linear feature extraction method, PCA uses global spectral information; it is widely used by researchers [3,4,46]. BP-ANN model obtained the best performance when FDs = 90, the accuracy of 5-fold cross validation and testing sets is 92.62% and 95.00%, respectively. With the softmax model, no matter how the FDs changes, the accuracy of 5-fold cross validation set was no less than 90.00%. The first ten principal components accounted for 98.95% of total variance. Moreover, the total variance reached 99.80%, when the first 90 PCs were used.

It is easier to achieve good performance with the CNN method. For example, the accuracy of 5-fold cross validation when the CNN method was used with the softmax classifier was higher than that of the validation set when other feature extraction methods were used for most feature dimensionality (except FDs = 10 and 40). In particular, when FD = 80, the accuracy of 5-fold cross validation was 96.67%, which was the highest accuracy achievable among all feature extraction methods. The accuracy of testing set even reach 98.57% with this parameter. The same phenomenon was observed with the BP-ANN classifier. When FDs = 10, 20, 30, 40, 80, the CNN method obtain a better accuracy of the 5-fold cross validation than other method. Even with other FDs, the accuracy of 5-fold cross validation was the second higher among all feature extraction methods.

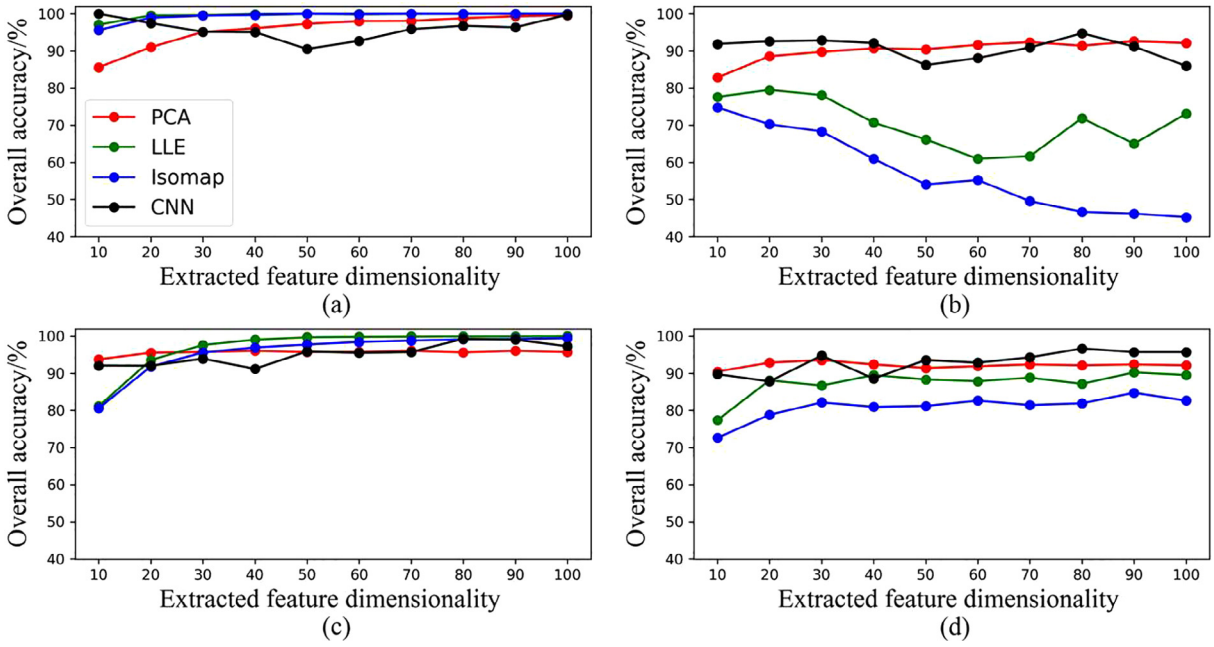

Fig. 5. Overall accuracy rates based on different feature extraction methods on feature dimensionality. (a) Calibration set with BP-ANN model, (b) 5-fold cross validation with BP-ANN model, (c) calibration set with softmax model, (d) 5-fold cross validation with softmax model.

Table 2
Classification accuracy of four spectral feature extraction methods under different classification models (%).

Models	Feature extraction methods	FD	Calibration set	Validation set	Testing set
BP-ANN	PCA	90	99.35	92.62	95.00
	LLE	20	99.58	79.52	80.71
	Isomap	10	95.65	74.76	75.00
	CNN	80	96.31	94.76	92.86
softmax	PCA	30	95.71	93.57	95.00
	LLE	90	99.94	90.24	87.14
	Isomap	90	99.23	84.76	82.86
	CNN	80	99.29	96.67	98.57

These results indicated that the convolution-pooling structure in the CNN could extract the internal features from the spectral data effectively, which resulted in the CNN exhibiting better performance than traditional feature extraction methods. Moreover, a CNN network structure with a unique local receptive field and weight sharing can reduce the number of parameters and increase robustness. In summary, we showed that the prediction performance when using a CNN for feature extraction was superior to that when using traditional methods such as the PCA, ISOMAP, and LLE for feature extraction. Some studies have also used spectral technology to evaluate tea quality. The CNN-softmax method proposed in this study has better accuracy than the variable iterative space shrinkage approach-artificial bee colony-support vector machine (VISSA-ABC-SVM) method with the accuracy of 97.44%, but the material has only three grades [47]. Ren et al. compared four different cognitive methods which are used to select characteristic wavelength variables [39]. Most of the method in this study obtained lower accuracy than CNN-softmax method. The highest accuracy of 99.01% was obtained with the method competitive adaptive reweighted sampling-least squares support vector machine (CARS-LSSVM), only slightly more than 98.57% obtained in this study. This is mainly since the CNN model can reduce irrelevant data and provide the classification model with more useful information. The classification model based on CNN was the most stable and had the highest classification accuracy of these four methods. By obtaining the spectral features of the network, the CNN model can reduce irrelevant data, and improve the generalization ability.

3.3. Appearance feature data description

A sample of Keemun black tea is depicted in Fig. 6. Directly distinguishing between tea samples of different grades is typically difficult because all samples are wiry. We analysed the geometric (shape) distribution of the samples of different grades and Fig. 7 illustrates box plots of the geometric features of the tea samples. We noted an overlap in the distribution ranges of the geometric features of the samples of various grades, particularly those of samples of adjacent grades. These results are consistent with those obtained for the appearance of the samples.

As indicated in the box plots, the median leaf width and length increased gradually as the tea grade decreased, and the distribution range of the upper and lower limits of the data tended to increase. According to sensory evaluation standards, high-grade black tea has slender leaves and more uniform texture than does low-grade tea. Accordingly, the observed distribution of the mentioned features is consistent with such sensory evaluation standards.

Fig. 7(c) and (d) display box plots of leaf area and perimeter, respectively. As the tea sample grade decreased, the median leaf

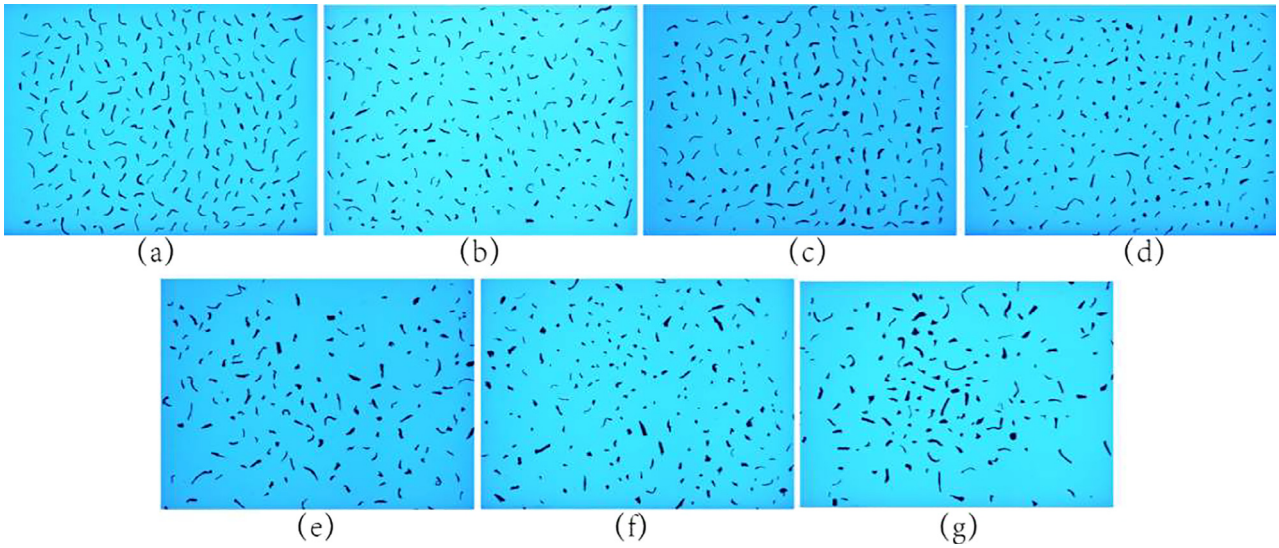

Fig. 6. Seven grades of tea images. (a) Super fine, (b) special grade, (c) first grade, (d) second grade, (e) third grade, (f) fourth grade, and (g) fifth grade.

area and perimeter of all samples, except for the fifth-grade sample, decreased first and then increased; the first-grade tea sample had the lowest median leaf area and perimeter. The reason for this phenomenon is that high-grade samples typically have more slender leaves than do low-grade samples. Compared with the high-grade samples (super fine and special grade), the first-grade tea samples used in this study contained a certain amount of crushed tea; this thus explains the decrease in the median leaf area and perimeter. However, as the grade decreased further, the leaves were noted to become wider, resulting in a gradual increase in the median leaf area and perimeter.

We determined that the four features of the fifth-grade sample did not conform to the general distribution observed in this study. The main reason could be that fifth-grade tea has the lowest quality requirement. To avoid wasting raw materials, manufacturers often combine the remaining raw materials of other grades to obtain fifth-grade tea, thus resulting in fifth-grade tea having more outlier points.

3.4. Discriminant result based on appearance feature

In order to obtain the discriminant results with different classifiers, the BP-ANN and softmax classifiers were used as the classification models. As shown in Table 3, when the BP-ANN was used as the classification model, the 5-fold cross validation accuracy and the testing accuracy were 67.38% and 70.71%, respectively. This is not an acceptable result. The possible reason for this is that the multilayer perceptron neural network applied a complex nonlinear function to fit the shape features. However, the shape feature histograms of each tea grade were similar, especially those of tea samples of adjacent grades. Therefore, it was difficult to fit the shape features accurately, which may be the reason for the low accuracy in grading.

When softmax was used as the classification model, the results significantly improved. The 5-fold cross validation accuracy for the validation set was 80.95%. The accuracy for the testing set was 85.71%. It was a moderate improvement over the accuracy achieved when the BP-ANN was used. The softmax classifier based on probability estimation used the minimised cross-entropy cost function to avoid the risk of falling into a local minimum in the gradient descent [48]. The results showed that the softmax classifier can obtain better classification results.

3.5. Discriminant result of data fusion

Among the spectral features obtained with each spectral feature extraction method, the spectral feature with the highest 5-fold cross validation accuracy was selected as the optimal feature. This spectral feature was fused with the shape feature into a new signal through a data vector. Then, the BP-ANN or softmax was applied to the fusion data sets to build the classification models. The classification results after feature fusion are summarised in Table 4. When BP-ANN classifier was used, the 5-fold cross validation accuracy of fusion feature was higher than that of a single sensor no matter what feature extraction method was used. When the fused feature contained a CNN processed NIRS feature, it can always obtain the best performance under different classifiers. The 5-fold cross validation and testing set accuracy based on the BP-ANN classifier were 97.86% and 96.43%, respectively. The accuracy of the 5-fold cross validation and testing set based on the softmax classifier was even reached to 99.29% and 100.00%, respectively.

Table 5 lists the 5-fold cross validation accuracy for each tea grade when using the softmax classifier. Only for shape feature classification, the mean accuracy of 5-fold cross validation was 80.95%; the accuracy for each grade was 81.67%, 76.67%, 71.67%, 91.67%, 83.33%, 76.67%, and 85.00%. The mean accuracy of 5-fold cross validation of NIRS features processed by the ISOMAP method was 84.76%; the accuracy for each grade was 93.33%, 83.33%, 76.67%, 91.67%, 85.00%, 76.67%, and 86.67%. The mean accuracy of 5-fold cross validation when data were fused increased to 91.67%; this was obtained by fusing NIRS features and shape features processed with ISOMAP. The classification accuracy obtained with the fused features was 95.00%, 90.00%, 85.00%, 96.67%, 96.67%, 88.33%, and 90.00%. We observed that the classification accuracy of all grade was improved after data fusion based on ISOMAP-processed NIRS and shape features. We also observed that the classification accuracy obtained with the fusion of NIRS features processed with the CNN was higher than that when using a single sensor feature. The classification accuracy of four grades was even reached 100%. The results showed that the accuracy of detailed classification was greatly improved. Similarly, the classification accuracy obtained with the fusion of PCA- or LLE-processed NIRS and shape features were also improved for the majority grade. Independent testing set classification accuracy for each tea grade also illustrated this phenomenon, as shown in Table 6.

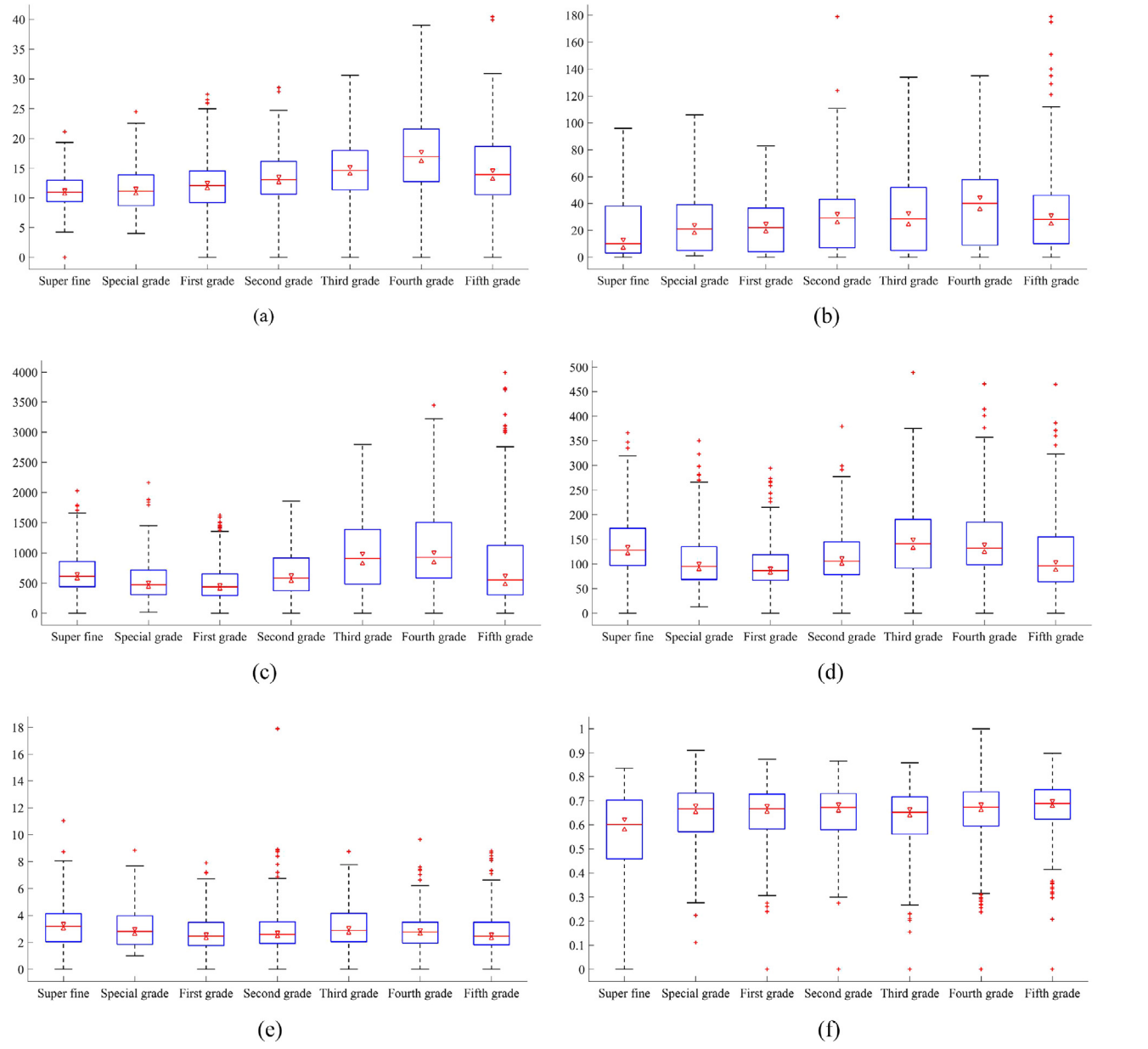

Fig. 7. Box plots of shape features. (a) leaf width, (b) leaf length, (c) leaf area, (d) leaf perimeter, (e) aspect ratio, and (f) rectangularity.

Table 3
The classification results of shape feature of Keemun black tea (%).

Models	Calibration set	Validation set	Testing set
BP-ANN	87.32	67.38	70.71
softmax	97.50	80.95	85.71

The results show that through the feature-level fusion strategy, the information from NIRS and CVS has a synergistic effect; the fusion results integrated the appearance information and endogenous characteristics of tea [34,48]. Therefore, it was clear that information features from a single sensor cannot distinguish between different tea grades effectively and accurately. Appearance, taste, aroma, and other factors should be considered for evaluating black tea quality.

The fusion of data obtained from various sensors can help evaluate multiple quality factors together; this would not be possible with data obtained from a single sensor. Feature-level data fusion (i.e. data obtained from multiple sources and fused) can help obtain a significantly higher accuracy than data obtained from a single sensor; feature-level data fusion can help achieve a classification accuracy up to 99.29%, and it has practical applications.

Some studies have also reported better performance of data fusion strategy. Li et al. evaluated green tea quality combing hyperspectral imaging and olfactory system. With the SVM classification model, the accuracy of the method reached 92.00% [49]. In comparison, this study obtained even higher classification accuracy. Xu, Wang, and Gu compared the performance of feature-level and decision-level fusion strategy [34]. The decision-level fusion, combining the SVM results of both E-nose and computer vision system, was the most effective strategy with the classification accuracy rates of 100.00%. The results of the current study show that the fusion data obtained better performance than the use of signal sensor alone.

Table 4
The total classification results of BP-ANN and softmax models based on feature-level fusion (%).

Models	Data source	Feature dimensionality	Calibration set	Validation set	Testing set
BP-ANN	CVS	92	87.32	67.38	70.71
	$NIRS^{(1)}$	90	99.35	92.62	95.00
	$NIRS^{(1)}$_CVS	182(90 + 92)	100.00	95.48	96.43
	$NIRS^{(2)}$	20	99.58	79.52	80.71
	$NIRS^{(2)}$_CVS	112(20 + 92)	95.12	84.52	86.43
	$NIRS^{(3)}$	10	91.90	74.76	75.00
	$NIRS^{(3)}$_CVS	102(10 + 92)	93.57	79.52	89.29
	$NIRS^{(4)}$	80	96.31	94.76	92.86
	$NIRS^{(4)}$_CVS	172(80 + 92)	99.95	97.86	96.43
softmax	CVS	92	97.50	80.95	85.71
	$NIRS^{(5)}$	30	95.71	93.57	95.00
	$NIRS^{(5)}$_CVS	122(30 + 92)	100.00	95.71	97.14
	$NIRS^{(6)}$	90	99.94	90.24	87.14
	$NIRS^{(6)}$_CVS	182(90 + 92)	100.00	92.62	97.86
	$NIRS^{(7)}$	90	99.23	84.76	82.86
	$NIRS^{(7)}$_CVS	182(90 + 92)	100.00	91.67	94.29
	$NIRS^{(8)}$	80	99.29	96.67	98.57
	$NIRS^{(8)}$_CVS	172(80 + 92)	100.00	99.29	100.00

CVS is the shape histograms feature. $NIRS^{(i)}$ is the NIRS feature with different feature extraction methods. $NIRS^{(i)}$_CVS is the fusion feature of shape feature and NIRS feature which extract by different methods.
i = 1, 5 are the NIRS features with the highest classification accuracy after the PCA process, which with BP-ANN and softmax classifier respectively.
i = 2, 6 are the NIRS features with the highest classification accuracy after the LLE process, which with BP-ANN and softmax classifier respectively.
i = 3, 7 are the NIRS features with the highest classification accuracy after ISOMAP process, which with BP-ANN and softmax classifier respectively.
i = 4, 8 are the NIRS features with the highest classification accuracy after CNN process, which with BP-ANN and softmax classifier respectively.

Table 5
The 5-fold cross validation set detail classification results of softmax model based on single sensor feature and feature-level fusion (%).

Data source	Super fine	Special grade	First grade	Second grade	Third grade	Fourth grade	Fifth grade	Mean accuracy
CVS	81.67	76.67	71.67	91.67	83.33	76.67	85.00	80.95
$NIRS^{(5)}$	96.67	93.33	95.00	100.00	88.33	85.00	96.67	93.57
$NIRS^{(5)}$_CVS	98.33	90.00	93.33	98.33	100.00	93.33	96.67	95.71
$NIRS^{(6)}$	86.67	91.67	88.33	95. 00	88.33	86.67	95.00	90.24
$NIRS^{(6)}$_CVS	90.00	83.33	88.33	98.33	98.33	93.33	96.67	92.62
$NIRS^{(7)}$	93.33	83.33	76.67	91.67	85.00	76.67	86.67	84.76
$NIRS^{(7)}$_CVS	95.00	90.00	85.00	96.67	96.67	88.33	90.00	91.67
$NIRS^{(8)}$	98.33	100.00	98.33	98.33	95.00	88.33	98.33	96.67
$NIRS^{(8)}$_CVS	98.33	100.00	98.33	100.00	100.00	98.33	100.00	99.29

CVS is the shape histograms feature. $NIRS^{(i)}$ is the NIRS feature with different feature extraction methods.
$NIRS^{(i)}$_CVS is the fusion feature of shape histograms feature and NIRS feature which extract by different methods.
i = 5 is the NIRS features with the highest classification accuracy after the PCA process, which with softmax classifier.
i = 6 is the NIRS features with the highest classification accuracy after the LLE process, which with softmax classifier.
i = 7 is the NIRS features with the highest classification accuracy after ISOMAP process, which with softmax classifier.
i = 8 is the NIRS features with the highest classification accuracy after CNN process, which with softmax classifier.

Table 6
The testing set detail classification results of softmax model based on single sensor feature and feature-level fusion (%).

Data source	Super fine	Special grade	First grade	Second grade	Third grade	Fourth grade	Fifth grade	Mean accuracy
CVS	80.00	75.00	100.00	90.00	95.00	80.00	80.00	85.71
$NIRS^{(5)}$	100.00	85.00	100.00	100.00	85.00	95.00	100.00	95.00
$NIRS^{(5)}$_CVS	95.00	95.00	95.00	100.00	95.00	100.00	100.00	97.14
$NIRS^{(6)}$	75.00	90.00	70. 00	100. 00	90. 00	85. 00	100. 00	87.14
$NIRS^{(6)}$_CVS	100.00	100.00	95.00	100.00	100.00	95.00	95.00	97.86
$NIRS^{(7)}$	75.00	65.00	80.00	95.00	95.00	75.00	95.00	82.86
$NIRS^{(7)}$_CVS	85.00	85.00	90.00	100.00	100.00	100.00	100.00	94.29
$NIRS^{(8)}$	100.00	95.00	100.00	100.00	100.00	100.00	95.00	98.57
$NIRS^{(8)}$_CVS	100.00	100.00	100.00	100.00	100.00	100.00	100.00	100.00

CVS is the shape histograms feature. $NIRS^{(i)}$ is the NIRS feature with different feature extraction methods.
$NIRS^{(i)}$_CVS is the fusion feature of shape histograms feature and NIRS feature which extract by different methods.
i = 5 is the NIRS feature with the highest classification accuracy after the PCA process, which with softmax classifier.
i = 6 is the NIRS feature with the highest classification accuracy after the LLE process, which with softmax classifier.
i = 7 is the NIRS feature with the highest classification accuracy after ISOMAP process, which with softmax classifier.
i = 8 is the NIRS feature with the highest classification accuracy after CNN process, which with softmax classifier.

4. Conclusion

This study verified the feasibility of using NIRS and CVS technology in combination with machine learning technology to assess the quality of Keemun black tea. Four feature extraction methods were compared in this study. The results showed that the CNN method has a higher prediction performance than the other methods. The most accurate results were obtained when CNN-processed NIRS features were classified using the softmax model. An extraction shape features scheme was proposed. We obtained histograms of the shape features to distinguish between the grades of tea samples. The softmax classifier based on the cross-entropy cost function yielded better classification results than the BP-ANN classifier. The developed feature-level fusion strategy synergistically integrates the advantages of NIRS and CVS information features. Fusion feature has a higher effect than a single sensor information feature in evaluating the quality of Keemun black tea. The classification of fusion features based on CNN-processed NIRS yielded the best result with softmax classification. In general, the method proposed in this study (i.e. the method of fusing NIRS and CVS information features) is suitable for assessing Keemun black tea quality. In order to apply this study to practice, more samples from different manufacturers and longer time span will be collected. With these additional data, the classification model, especially the deep learning model, will be further optimized.

CRediT authorship contribution statement

Yan Song: Conceptualization, Data curation, Formal analysis, Writing - review & editing, Funding acquisition, Project administration. **Xiaozhong Wang:** Data curation, Software, Investigation, methodology, Validation, Visualization, Writing - original draft. **Hanlei Xie:** Investigation, Methodology. **Luqing Li:** Writing - review & editing. **Jingming Ning:** Writing - review & editing, Funding acquisition, Project administration. **Zhengzhu Zhang:** Writing - review & editing, Funding acquisition, Project administration.

Declaration of Competing Interest

The authors declare that they have no known competing financial interests or personal relationships that could have appeared to influence the work reported in this paper.

Acknowledgements

The present study was financially supported by Primary Research and Development Plan of Anhui Province (201904a06020006), the Major Science and Technology Projects of Anhui Province (18030701153), National Key Laboratory Open Fund Project (Open Fund of State Key Laboratory of Tea Plant Biology and Utilization, Anhui Agricultural University, SKLTOF20170118), and National Key Research and Development Plan Project (2017YFD0400800).

References

[1] S. Kang, H. Yan, Y. Zhu, X. Liu, H.P. Lv, Y. Zhang, W.D. Dai, L. Guo, J.F. Tan, Q.H. Peng, Z. Lin, Identification and quantification of key odorants in the world's four most famous black teas, Food Res. Int. 121 (2019) 73–83, https://doi.org/10.1016/j.foodres.2019.03.009.

[2] R. Zhi, L. Zhao, D. Zhang, A framework for the multi-level fusion of electronic nose and electronic tongue for tea quality assessment, Sensors (Basel) 17 (5) (2017) 1007, https://doi.org/10.3390/s17051007.

[3] A. Shevchuk, L. Jayasinghe, N. Kuhnert, Differentiation of black tea infusions according to origin, processing and botanical varieties using multivariate statistical analysis of LC-MS data, Food Res. Int. 109 (2018) 387–402, https://doi.org/10.1016/j.foodres.2018.03.059.

[4] C. Ma, J. Li, W. Chen, W. Wang, D. Qi, S. Pang, A. Miao, Study of the aroma formation and transformation during the manufacturing process of oolong tea by solid-phase micro-extraction and gas chromatography-mass spectrometry combined with chemometrics, Food Res. Int. 108 (2018) 413–422, https://doi.org/10.1016/j.foodres.2018.03.052.

[5] H.T. Zhao, Y.Z. Feng, W. Chen, G.F. Jia, Application of invasive weed optimization and least square support vector machine for prediction of beef adulteration with spoiled beef based on visible near-infrared (Vis-NIR) hyperspectral imaging, Meat Sci. 151 (2019) 75–81, https://doi.org/10.1016/j.meatsci.2019.01.010.

[6] M.J. Aliano-Gonzalez, M. Ferreiro-Gonzalez, E. Espada-Bellido, M. Palma, G.F. Barbero, A screening method based on Visible-NIR spectroscopy for the identification and quantification of different adulterants in high-quality honey, Talanta 203 (2019) 235–241, https://doi.org/10.1016/J.TALANTA.2019.05.067.

[7] S. Tian, J. Zhang, Z. Zhang, J. Zhao, Z. Zhang, H. Zhang, Effective modification through transmission Vis/NIR spectra affected by fruit size to improve the prediction of moldy apple core, Infrared Phys. Technol. 100 (2019) 117–124, https://doi.org/10.1016/j.infrared.2019.05.015.

[8] L.F. Santos Pereira, S. Barbon, N.A. Valous, D.F. Barbin, Predicting the ripening of papaya fruit with digital imaging and random forests, Comput. Electron. Agric. 145 (2018) 76–82, https://doi.org/10.1016/j.compag.2017.12.029.

[9] J. Wang, Y. Wang, J. Cheng, J. Wang, X. Sun, S. Sun, Z. Zhang, Enhanced cross-category models for predicting the total polyphenols, caffeine and free amino acids contents in Chinese tea using NIR spectroscopy, Lwt 96 (2018) 90–97, https://doi.org/10.1016/j.lwt.2018.05.012.

[10] Y.J. Fan, Autoencoder node saliency: Selecting relevant latent representations, Pattern Recogn. 88 (2019) 643–653, https://doi.org/10.1016/j.patcog.2018.12.015.

[11] J.P. Reed, D. Devlin, S.R. Esteves, R. Dinsdale, A.J. Guwy, Integration of NIRS and PCA techniques for the process monitoring of a sewage sludge anaerobic digester, Bioresour. Technol. 133 (2013) 398–404, https://doi.org/10.1016/j.biortech.2013.01.083.

[12] W. Zhou, H. Liu, Q. Xu, P. Li, L. Zhao, H. Gao, Glycerol's generalized two-dimensional correlation IR/NIR spectroscopy and its principal component analysis, Spectrochim. Acta A Mol. Biomol. Spectrosc. 228 (2020) 117824, https://doi.org/10.1016/j.saa.2019.117824.

[13] M. Huang, Q. Zhu, B. Wang, R. Lu, Analysis of hyperspectral scattering images using locally linear embedding algorithm for apple mealiness classification, Comput. Electron. Agric. 89 (2012) 175–181, https://doi.org/10.1016/j.compag.2012.09.003.

[14] W. Sun, A. Halevy, J.J. Benedetto, W. Czaja, C. Liu, H. Wu, B. Shi, W. Li, UL-Isomap based nonlinear dimensionality reduction for hyperspectral imagery classification, ISPRS J. Photogramm. Remote Sens. 89 (2014) 25–36, https://doi.org/10.1016/j.isprsjprs.2013.12.003.

[15] P. Mishra, A. Nordon, J. Tschannerl, G. Lian, S. Redfern, S. Marshall, Near-infrared hyperspectral imaging for non-destructive classification of commercial tea products, J. Food Eng. 238 (2018) 70–77.

[16] K.P. Ferentinos, Deep learning models for plant disease detection and diagnosis, Comput. Electron. Agric. 145 (2018) 311–318, https://doi.org/10.1016/j.compag.2018.01.009.

[17] A. Farooq, J. Hu, X. Jia, Analysis of spectral bands and spatial resolutions for weed classification via deep convolutional neural network, IEEE Geosci. Remote Sens. Lett. 16 (2) (2019) 183–187, https://doi.org/10.1109/LGRS.2018.2869879.

[18] X. Cheng, Y. Zhang, Y. Chen, Y. Wu, Y. Yue, Pest identification via deep residual learning in complex background, Comput. Electron. Agric. 141 (2017) 351–356, https://doi.org/10.1016/j.compag.2017.08.005.

[19] G.S. Gill, A. Kumar, R. Agarwal, Nondestructive grading of black tea based on physical parameters by texture analysis, Biosyst. Eng. 116 (2) (2013) 198–204, https://doi.org/10.1016/j.biosystemseng.2013.08.002.

[20] H. Zhu, Y. Ye, H. He, C. Dong, Evaluation of green tea sensory quality via process characteristics and image information, Food Bioprod. Process. 102 (2017) 116–122, https://doi.org/10.1016/j.fbp.2016.12.004.

[21] J. Miao, Z. Luo, Y. Wang, G. Li, Comparison and data fusion of an electronic nose and near-infrared reflectance spectroscopy for the discrimination of ginsengs, Anal. Methods 8 (6) (2016) 1265–1273, https://doi.org/10.1039/C5AY03270A.

[22] S. Kiani, S. Minaei, M. Ghasemi-Varnamkhasti, Integration of computer vision and electronic nose as non-destructive systems for saffron adulteration detection, Comput. Electron. Agric. 141 (2017) 46–53, https://doi.org/10.1016/j.compag.2017.06.018.

[23] Å. Rinnan, F.V.D. Berg, S.B. Engelsen, Review of the most common pre-processing techniques for near-infrared spectra, TrAC-Trends, Anal. Chem. 28 (10) (2009) 1201–1222, https://doi.org/10.1016/j.trac.2009.07.007.

[24] P. Nie, J. Zhang, X. Feng, C. Yu, Y. He, Classification of hybrid seeds using near-infrared hyperspectral imaging technology combined with deep learning, Sens. Actuators, B 296 (2019) 126630, https://doi.org/10.1016/j.snb.2019.126630.

[25] J. Jiao, M. Zhao, J. Lin, J. Zhao, A multivariate encoder information based convolutional neural network for intelligent fault diagnosis of planetary gearboxes, Knowl.-Based Syst. 160 (2018) 237–250, https://doi.org/10.1016/j.knosys.2018.07.017.

[26] J. Gu, Z. Wang, J. Kuen, L. Ma, A. Shahroudy, B. Shuai, T. Liu, X. Wang, G. Wang, J. Cai, T. Chen, Recent advances in convolutional neural networks, Pattern Recogn. 77 (2018) 354–377, https://doi.org/10.1016/j.patcog.2017.10.013.

[27] N. Srivastava, G. Hinton, A. Krizhevsky, I. Sutskever, R. Salakhutdinov, Dropout: A simple way to prevent neural networks from overfittin, J. Mach. Learn. Res. 15 (2014) 1929–1958.

[28] L. Matten, E. Postma, J. Herik, Dimensionality Reduction: A Comparative Review. Tillburg University Technical Report, TICC-TR 2009-005.
[29] C. Lu, P. Zhu, Y. Cao, The segmentation algorithm of improvement a two-dimensional Otsu and application research, in: 2010 2nd International Conference on Software Technology and Engineering, 1(2010) 76–79. https://doi.org/10.1109/ICSTE.2010.5608908.
[30] A. Aakif, M.F. Khan, Automatic classification of plants based on their leaves, Biosyst. Eng. 139 (2015) 66–75, https://doi.org/10.1016/j.biosystemseng.2015.08.003.
[31] G. Saleem, M. Akhtar, N. Ahmed, W.S. Qureshi, Automated analysis of visual leaf shape features for plant classification, Comput. Electron. Agric. 157 (2019) 270–280, https://doi.org/10.1016/j.compag.2018.12.038.
[32] T. Munisami, M. Ramsurn, S. Kishnah, S. Pudaruth, Plant leaf recognition using shape features and colour histogram with K-nearest neighbour classifiers, Procedia Comput. Sci. 58 (2015) 740–747, https://doi.org/10.1016/j.procs.2015.08.095.
[33] X. Zhao, Z. He, S. Zhang, D. Liang, Robust pedestrian detection in thermal infrared imagery using a shape distribution histogram feature and modified sparse representation classification, Pattern Recogn. 48 (6) (2015) 1947–1960, https://doi.org/10.1016/j.patcog.2014.12.013.
[34] M. Xu, J. Wang, S. Gu, Rapid identification of tea quality by E-nose and computer vision combining with a synergetic data fusion strategy, J. Food Eng. 241 (2019) 10–17, https://doi.org/10.1016/j.jfoodeng.2018.07.020.
[35] E. Kaya, İ. Saritas, Towards a real-time sorting system: Identification of vitreous durum wheat kernels using ANN based on their morphological, colour, wavelet and gaborlet features, Comput. Electron. Agric. 166 (2019) 105016, https://doi.org/10.1016/j.compag.2019.105016.
[36] Z. Chen, J. Cheng, A parallel Softmax classification algorithm based on MapReduce, in: The 13th International Conference on Computer Science and Education (ICCSE 2018), (2018) 8-11.
[37] J. Sun, Y. Zhang, H. Mao, S. Cong, X. Wu, P. Wang, Research of moldy tea identification based on RF-RFE-Softmax model and hyperspectra, Optik – Int. J. Light Electron Optics 153 (2018) 156–163, https://doi.org/10.1016/j.ijleo.2017.10.020.
[38] Q. Chen, J. Zhao, C.H. Fang, D. Wang, Feasibility study on identification of green, black and Oolong teas using near-infrared reflectance spectroscopy based on support vector machine (SVM), Spectrochim. Acta A Mol. Biomol. Spectrosc. 66 (3) (2007) 568–574, https://doi.org/10.1016/j.saa.2006.03.038.
[39] G. Ren, Y. Wang, J. Ning, Z. Zhang, Highly identification of keemun black tea rank based on cognitive spectroscopy: Near infrared spectroscopy combined with feature variable selection, Spectrochim. Acta A Mol. Biomol. Spectrosc. 230 (2020) 118079, https://doi.org/10.1016/j.saa.2020.118079.
[40] Q. Chen, D. Zhang, W. Pan, Q. Ouyang, H. Li, K. Urmila, J. Zhao, Recent developments of green analytical techniques in analysis of tea's quality and nutrition, Trends Food Sci. Technol. 43 (1) (2015) 63–82, https://doi.org/10.1016/j.tifs.2015.01.009.
[41] A.B.S.d. Lima, A.S. Batista, J.C.d. Jesus, J.d.J. Silva, A.C.M.d. Araújo, L.S. Santos, Fast quantitative detection of black pepper and cumin adulterations by near-infrared spectroscopy and multivariate modeling, Food Control 107 (2020) 106802, https://doi.org/10.1016/j.foodcont.2019.106802.
[42] G.e. Jin, Y. Wang, L. Li, S. Shen, W.-W. Deng, Z. Zhang, J. Ning, Intelligent evaluation of black tea fermentation degree by FT-NIR and computer vision based on data fusion strategy, Lwt 125 (2020) 109216, https://doi.org/10.1016/j.lwt.2020.109216.
[43] Y.-J. Wang, T.-H. Li, L.-Q. Li, J.-M. Ning, Z.-Z. Zhang, Micro-NIR spectrometer for quality assessment of tea: Comparison of local and global models, Spectrochim. Acta A Mol. Biomol. Spectrosc. 237 (2020) 118403, https://doi.org/10.1016/j.saa.2020.118403.
[44] T. Liu, Z. Li, C. Yu, Y. Qin, NIRS feature extraction based on deep auto-encoder neural network, Infrared Phys. Technol. 87 (2017) 124–128, https://doi.org/10.1016/j.infrared.2017.07.015.
[45] S. Wang, S. Liu, J. Zhang, X. Che, Z. Wang, D. Kong, Feasibility study on prediction of gasoline octane number using NIR spectroscopy combined with manifold learning and neural network, Spectrochim. Acta A Mol. Biomol. Spectrosc. 228 (2020) 117836, https://doi.org/10.1016/j.saa.2019.117836.
[46] C. Pasquini, Near-infrared spectroscopy: A mature analytical technique with new perspectives - A review, Anal. Chim. Acta 1026 (2018) 8–36, https://doi.org/10.1016/j.aca.2018.04.004.
[47] Y. Li, J. Sun, X. Wu, B. Lu, M. Wu, C. Dai, Grade identification of Tieguanyin tea using fluorescence hyperspectra and different statistical algorithms, J. Food Sci. 84 (2019) 2234–2241.
[48] Goodfellow et al. Deep Learning. MIT Press, 2016. http://www.deeplearningbook.org.
[49] L. Li, S. Xie, J. Ning, Q. Chen, Z. Zhang, Evaluating green tea quality based on multisensor data fusion combining hyperspectral imaging and olfactory visualization systems, J. Sci. Food Agric. 99 (4) (2019) 1787–1794, https://doi.org/10.1002/jsfa.2019.99.issue-410.1002/jsfa.9371.